Advances in Radiation Oncology (2020) **5**, 1022-1031

advances
in radiation oncology

www.advancesradonc.org

Scientific Article

Multiple Computed Tomography Robust Optimization to Account for Random Anatomic Density Variations During Intensity Modulated Proton Therapy

Mingyao Zhu, PhD,[a,*,1] Adeel Kaiser, MD,[a] Mark V. Mishra, MD,[a] Young Kwok, MD,[a] Jill Remick, MD,[b] Cristina DeCesaris, MD,[b] and Katja M. Langen, PhD[a,1]

[a]Department of Radiation Oncology, Maryland Proton Treatment Center, University of Maryland School of Medicine, Baltimore, Maryland; and [b]Department of Radiation Oncology, University of Maryland Medical Center, Baltimore, Maryland

Received 8 October 2019; revised 4 December 2019; accepted 12 December 2019

Abstract

Purpose: To propose a method of optimizing intensity modulated proton therapy (IMPT) plans robust against dosimetric degradation caused by random anatomic variations during treatment.

Methods and Materials: Fifteen patients with prostate cancer treated with IMPT to the pelvic targets were nonrandomly selected. On the repeated quality assurance computed tomography (QACTs) for some patients, bowel density changes were observed and caused dose degradation because the treated plans were not robustly optimized (non-RO). To mitigate this effect, we developed a robust planning method based on 3 CT images, including the native planning CT and its 2 copies, with the bowel structures being assigned to air and tissue, respectively. The RO settings included 5 mm setup uncertainty and 3.5% range uncertainty on 3 CTs. This method is called pseudomultiple-CT RO (pMCT-RO). Plans were also generated using RO on the native CT only, with the same setup and range uncertainties. This method is referred to as single-CT RO (SCT-RO). Doses on the QACTs and the nominal planning CT were compared for the 3 planning methods.

Results: All 3 plan methods provided sufficient clinical target volumes D95% and V95% on the QACTs. For pMCT-RO plans, the normal tissue D_{max} on QACTs of all patients was at maximum 109.1%, compared with 144.4% and 116.9% for non-RO and SCT-RO plans, respectively. On the nominal plans, the rectum and bladder doses were similar among all 3 plans; however, the volume of normal tissue (excluding the rectum and bladder) receiving the prescription dose or higher is substantially reduced in either pMCT-RO plans or SCT-RO plans, compared with the non-RO plans.

Conclusions: We developed a robust optimization method to further mitigate undesired dose heterogeneity caused by random anatomic changes in pelvic IMPT treatment. This method does not require additional patient CT scans. The pMCT-RO planning method has been implemented clinically since 2017 in our center.

Sources of support: This work had no specific funding.

Disclosures: Dr Mishra reports grants from ASTRO Comparative Effectiveness Grant, personal fees from Varian, other from GE Health care, and other from Adverum outside the submitted work. Dr Langen reports personal fees from Varian Medical outside of the submitted work.

* Corresponding author: Mingyao Zhu, PhD; E-mail: mingyao.zhu@emory.edu

[1] Current affiliation: Department of Radiation Oncology, School of Medicine, Emory University, Atlanta, Georgia

https://doi.org/10.1016/j.adro.2019.12.003

Introduction

Proton beam therapy is used to treat a variety of solid tumors.[1,2] The finite range of proton beams eliminates exit dose,[3] resulting in a reduction in integral dose of radiation and better sparing of organs at risk (OARs) in many cases.[4-9] However, the range of proton beams is subject to uncertainties that must be understood and accounted for in the treatment plan to avoid compromising clinical goals.[10]

Uncertainties in the Hounsfield units to relative stopping power calibration result in uncertainty of the proton range; a typical value of 2.5% to 3.5% with additional 1 to 3 mm is applied at most centers.[11] Proton beams are also uniquely sensitive to setup uncertainties because the dose distribution itself can change with variations in tissue density and water-equivalent depth along the beam's path. These two uncertainties are well understood and are accounted for in treatment planning with robustness evaluation or optimization.[12]

Systematic or random variations in the patient anatomy present an even more challenging scenario. Repeat computed tomography (CT) images can be acquired throughout the treatment course to assess the effect of these uncertainties. Systematic changes can be addressed with off-line adaptive radiation therapy, but random changes are more difficult to address. In our clinical practice we have observed, on repeat CT scans, plan degradations in intermediate- to high-risk prostate patients whose treatment volume includes pelvic nodal chains. Although the target was sufficiently covered, hot spots have been seen on repeat CTs owing to patient anatomy change. In similar cases, others reported that the proton dose distribution can change owing to variations in bowel filling.[9,13,14] Although online adaptive radiation therapy could be used to address this issue, this technology is not currently being used in clinical practice. We therefore investigated whether random anatomic changes can be addressed at time of treatment planning.

The use of multiple CT (mCT) scans to generate plans that are robust against systematic anatomic changes in patients with lung cancer and random cavity filling variation in patients with head and neck cancer have recently been investigated.[15,16] We hypothesized that this concept can be used to improve robustness against random anatomic density variations in patients with prostate cancer whose target volume includes pelvic nodes.

A pencil beam scanning planning technique based on multifield optimizations (MFO) and robust optimization (RO) on multiple CT scans was developed and evaluated for its ability to improve robustness against random anatomic variations. The set of multiple CT scans is composed of the native planning CT and 2 synthetic CTs that mimic anticipated anatomic changes. These plans were compared against standard MFO plans generated with and without RO. The dose to normal tissues was compared for each planning technique to assess the dosimetric cost of each technique.

Methods and Materials

Patient cohort

Fifteen patients with intermediate- to high-risk prostate cancer treated from June 2016 to April 2017 at our center were nonrandomly identified and reviewed under an institutional review board–approved protocol. All patients received intensity modulated proton therapy to the pelvic nodes to 45 to 46 Gy (1.8-2 Gy per fraction) followed by external beam or brachytherapy boost to the prostate. Proximal seminal vesicles were included in selected patients undergoing external beam radiation boost only.

Simulation and contouring

All patients completed a treatment planning simulation CT scan with 3-mm slice thickness from the bottom of the L1 vertebral body to midfemur. A comfortably full bladder and empty rectum were required for each scan. Customized immobilization devices were placed underneath patient legs, and knees and were indexed to the CT and treatment table. CT data was then imported into treatment planning software. Target tissues, including pelvic nodes, the prostate, and seminal vesicles were contoured using CT, and when available magnetic resonance images. Appropriate expansions were added to these structures to create clinical target volumes (CTV). In general, the nodal regions were created by adding a 7- to 8-mm margin around vessels, although the prostate and seminal vesicles were not expanded. Critical normal organs, including the bladder, rectum, femoral heads, small bowel, large bowel, and the penile bulb were subsequently contoured. All patients had fiducial markers implanted into the prostate, and these were also contoured to permit image guided delivery of external beam radiation.

Planning details of clinical plans: MFO without robustness optimization

A total dose of 45 to 46 Gy in 23 to 25 fractions was prescribed to the CTV. To account for uncertainties for this CTV region, a proton planning target volume (pPTV)

was constructed by expanding the CTV by 7 mm in the left, right, and anterior dimensions, and by adding a 5-mm margin in the superior, inferior, and posterior directions. The CTV and pPTV volumes on the planning CT are listed in Table 1 for the 15 patients. Figure 1a-c is an example of the CTV (red) and pPTV (magenta). A 3-field beam arrangement with 2 lateral fields (RL and LL) and a posterior-anterior (PA) field was used. The 7-mm expansion in the left, right, and anterior direction was chosen to account for a 3.5% range uncertainty for the RL, LL, and PA fields, respectively; and the 5-mm expansion in other directions was used to account for setup errors. The pPTV was partitioned into 3 partial target volumes for proton spot placement: pPTV_L, pPTV_R, and pPTV_PA for the LL, RL, and PA fields, respectively. Manual editing of contours was performed to ensure that the lateral beams did not cross midline in areas where the pPTV was separated by intermediate normal tissues, such as the bowel and bladder, with a distance of 3 cm or larger. The PA beam was designed to prevent passing through the rectum. At the level of the prostate and seminal vesicles the pPTV was covered only by 2 lateral beams. Figure 1d-l illustrates pPTV_R (blue), pPTV_L (cyan), and pPTV_PA (orange) contours at 3 different axial views, along with the field-dose distribution of the 3 beams. As seen in Figure 1, all portions of the pPTV are treated by at least 2 fields.

After all beam arrangements were completed, the treatment plan was optimized using a commercial treatment planning system (TPS) with MFO capability. Robustness optimization was not available in the TPS at time of planning and therefore the plans were optimized to achieve desired coverage of the pPTV. To cover the pPTV, additional 5- to 7-mm margins were added to the pPTV subvolumes for spot placement. This type of plan is referred to as non-RO plans. The 15 patients in this study were all treated with non-RO plans.

Rescan quality assurance CTs contouring and evaluation

Patients were rescanned weekly in the same position with the simulation CT scanner and the same immobilization devices. The number of available rescanned quality assurance CT images (QACTs) for each patient is listed in Table 1, and there were a total of 67 QACTs for the 15 patients. The QACTs were rigidly registered with the planning CT image set based on bony structure alignment, the treatment plan was recalculated on QACTs, and the dose distributions on the QACTs were evaluated. For the 15 patients in this study, the CTV, bladder, and rectum were contoured on the available 67 QACTs by physicians using the same institutional guidelines. Figure 2 illustrates

Table 1 Comparison of the D_{max} in the target proton pPTV and NT on the nominal plan and highest values among all weekly QACT scans of each patient for the 3 treatment planning methods

Pt. No.	No. of QACTs	CTV volume (mL)	pPTV volume (mL)	Non-RO				SCT-RO				pMCT-RO			
				Nominal Dmax (%)		QA Dmax (%)		Nominal Dmax (%)		QA Dmax (%)		Nominal Dmax (%)		QA Dmax (%)	
				pPTV	NT	pPTV	NT	pPTV	NT	pPTV	NT	pPTV	NT	pPTV	NT
1	3	292.4	640.8	105.8	105.6	**121.1**	**121.2**	106.2	104.0	106.9	107.1	106.6	106.4	107.9	106.7
2	4	519.6	961.4	105.4	103.8	**121.1**	**131.6**	109.9	106.7	**110.6**	**115.3**	107.0	106.1	109.2	109.1
3	4	473.0	952.3	106.7	106.1	**122.5**	**122.5**	105.7	103.9	106.9	106.9	105.9	104.7	108.0	106.8
4	4	566.4	1109.9	105.3	104.9	**122.2**	**144.4**	106.6	105.2	**112.4**	**116.9**	106.7	105.8	109.4	108.8
5	5	477.6	996.9	106.2	104.8	**126.5**	**133.4**	109.5	105.5	**110.8**	**110.7**	106.9	106.2	108.9	108.8
6	5	493.3	1003.2	105.2	104.2	**130.2**	**140.7**	106.8	104.7	**111.1**	**112.7**	105.5	105.3	106.9	109.1
7	5	384.8	862.6	105.9	105.6	**117.6**	**121.2**	109.6	106.0	**109.4**	**112.9**	106.0	105.8	107.0	109.0
8	4	250.1	630.2	104.3	104.2	**110.7**	**128.1**	107.2	105.0	109.9	109.9	106.5	106.0	108.6	107.8
9	5	507.6	1061.9	105.7	105.1	**115.2**	**122.3**	**110.1**	106.7	**110.2**	**112.3**	107.9	106.7	109.1	108.7
10	4	598.4	1194.5	108.3	107.1	**117.9**	**120.5**	104.7	103.7	107.8	108.9	105.1	104.8	107.7	107.2
11	5	663.3	1189.4	105.4	104.8	**110.2**	**119.8**	108.8	106.8	109.2	109.7	107.1	107.1	105.5	105.5
12	4	537.6	987.7	105.4	104.6	**116.7**	**119.3**	106.3	105.4	109.1	109.1	106.8	106.4	109.9	109.1
13	5	637.1	1164.1	**110.3**	106.6	**114.2**	**116.1**	106.7	104.8	108.9	109.0	106.4	105.8	**110.6**	108.8
14	5	417.8	886.1	**110.8**	107.0	**113.0**	**113.2**	106.5	105.0	107.3	107.5	106.1	105.6	**110.7**	109.0
15	5	503.7	1029.4	106.1	104.7	**111.5**	**111.5**	107.1	105.2	108.3	108.3	107.0	106.8	107.8	107.7
			Mean	106.5	105.3			107.4	105.2			106.5	106.0		
			STD	1.8	1.0			1.6	1.0			0.7	0.7		

The number of quality assurance computed tomographic scans, the clinical target volumes (CTV) volume and the PTV volume for each patient are also listed. The mean and standard deviation (STD) are calculated for the nominal plan doses.
Bold indicates maximum dose values greater than 110.0%
Abbreviations: Dmax = maximum point dose; NT = normal tissue; pPTV = proton planning target volume; QACT = quality assurance computed tomographic scans.

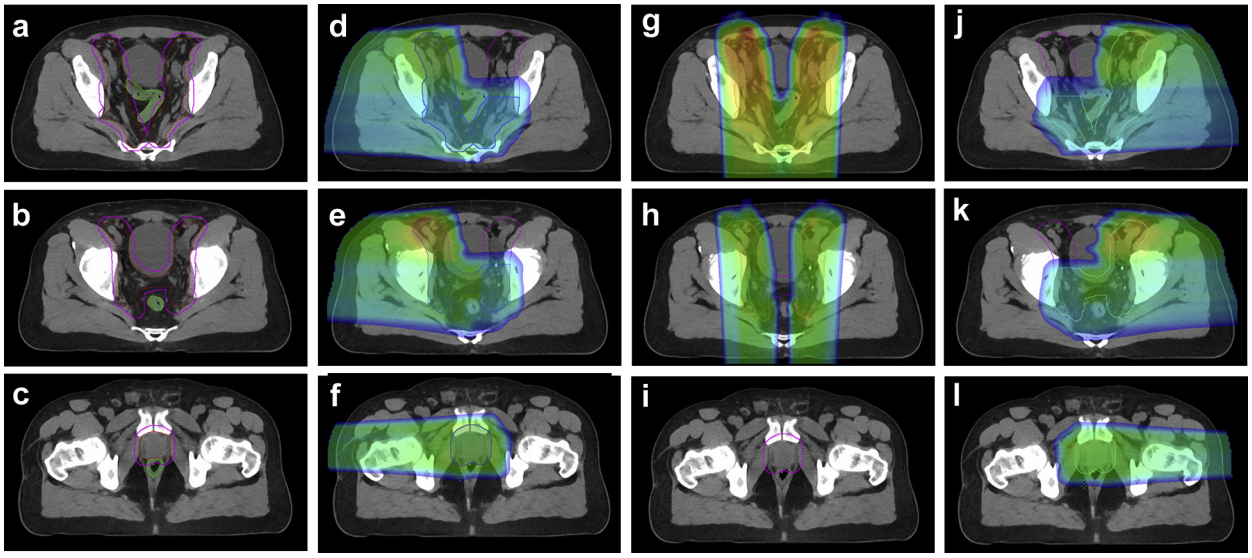

Figure 1 Clinical target volumes (red) and proton planning target volume (pPTV; magenta) for an example patient. The density of the green contour in (a-c) is assigned to air and tissue density on the computed tomography air and computed tomography tissue, respectively. The blue, orange, and cyan filled contour are the pPTV_RT, pPTV_PA, and pPTV_LT volumes. Typical field dose for the right-lateral (d-f), posterior-anterior (g-i), and left-lateral (j-l) beams demonstrates that superiorly, the 3 fields cover the pelvic nodes, with all portions of the target covered by at least 2 beams. Only the 2 lateral fields cover the prostate; the posterior-anterior beam (i) does not cover the target to avoid beam passing through the rectum.

the planning CT nominal dose along with the recalculated dose on a weekly QACT scan.

MFO plans with RO on multiple CT scans

Using the same planning CT image, beam arrangement, and pPTV subvolume partition as used clinically, different treatment plans were retrospectively generated for the same patient cohort. Because the coverage of CTV is robustly optimized, the pPTV coverage is not included in plan optimization. The pPTV subvolumes (with margin) were used to place proton spots for the corresponding fields. To simulate the potential anatomy and density changes due to bowel filling over time, 2 copies of the planning CT image are created from and registered to the planning CT. On the first copy, CT_air, the bowel structures, including the rectum, large bowel, and small bowel, were assigned a density of air to mimic potential gas bubble formation. On the second copy, CT_tissue, the identical bowel structures were assigned a density of soft tissue to mimic the absence of gas. For example, the density of the green contour (rectum and small bowel) shown in Fig 1a-c is assigned to air and tissue in the CT_air and CT_tissue images, respectively.

Using the 4-dimensional (4D) optimization feature in a commercial TPS, we included all 3 CT image sets in the robustness optimization process. The robustness optimization included 21 scenarios per CT, for a total of 63 scenarios using the planning CT, CT_air, and CT_tissue data sets. The 21 scenarios per CT incorporated a combination of 7 patient position scenarios (5 mm in 6 directions and the nominal position without shift) and 3 range uncertainty scenarios (positive and negative 3.5%, and the nominal range without offset).[17] Because the 3 CT image sets are all based on the one planning CT, we call this method pseudomultiple CT robustness optimization (pMCT-RO).[18] Table E1 (available online at https://doi.org/10.1016/j.adro.2019.12.003) shows the parameters used to optimize the pMCT-RO plans.

MFO plan with RO on native planning CT

Traditional robust optimization for setup and range uncertainties using 21 scenarios on only the native CT were tested for comparison. Because only one CT image set is used, we call this method single-CT RO (SCT-RO), to distinguish it from the pMTC-RO described in the previous section. The same patient setup and range uncertainty (5 mm and 3.5%) as in the pMCT-RO method were used. All relevant planning parameters were kept constant with the exception of excluding the synthetic CTs (CT_air and CT_tissue) from the RO process.

Dosimetric comparison between the 3 methods

For comparison purposes, the treated non-RO plans, SCT-RO plans, and pMCT-RO plans were normalized to D98 of the CTV receiving 45 Gy. The coverage of the CTV was also evaluated by comparing the CTV V95% (percent volume receiving 95% of the prescription dose or higher) and D95% (minimum dose to at least 95% of

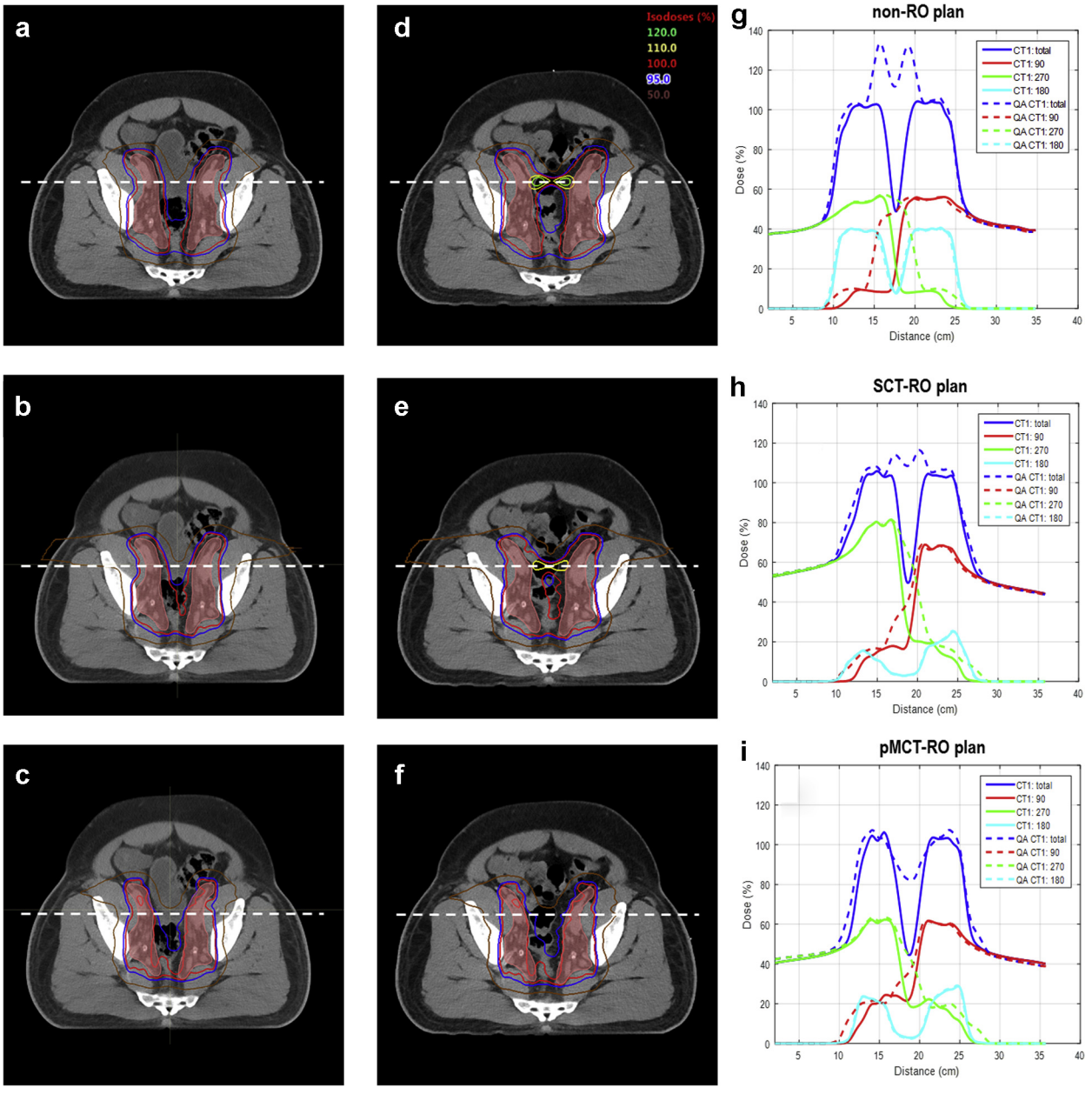

Figure 2 Dose distribution of the 3 planning methods: not robustly optimized (a, d), single computed tomography (CT) robustly optimized (b, e) and pseudomultiple CT robustly optimized (c, f) on the planning CT (a-c) and the rescanned quality assurance (QACT) (d-f). The pink color filled contour is the clinical target volumes (CTV) on the planning CT and the QACT. Corresponding total and beam dose profiles on planning CT and QACT along the dotted line are provided in (g-i).

the volume) on the dose-recalculated on QACTs among the 3 methods. Because improved robustness could be associated with higher OAR or normal tissue doses, we also compared the following OAR doses on the nominal plans and on the QACTs: rectum point maximum dose (D_{max}), rectum V90% (percent volume receiving 90% of prescription dose or higher), and bladder D_{max}, bladder V100% (percent volume receiving the prescription dose or higher). The D_{max} to the target (pPTV) and to the normal tissues (NT) outside of pPTV on the nominal plans and the QACTs was also compared. In addition, the absolute volume of remaining normal tissue of the pelvis (NT_p and NT_c) receiving the prescription dose or higher was compared for the nominal plans. The NT_p volume was defined as the patient body volume minus the sum of pPTV, bladder and rectum volumes; although the NT_c was defined in a similar way as NT_p but using CTV instead of pPTV. Paired 2-tail *t* test was used, with a *P* value less than .05 considered statistically significant.

Results

Dose to CTV on the QACTs

Table 2 lists the average and standard deviation of the CTV V95% and D95% on the 67 QACTs for each plan type, along with the *P* value of the comparison between plan types. Plots in Figure 3 compare all the CTV V95% and D95% values on QACTs among different planning methods, the solid lines indicate the 2 methods have same dose values. All 3 methods provided sufficient dose coverage to the CTV on QACTs as evaluated by D95% and V95%. There is no statistically significant difference for CTV D95% among the 3 methods. All 3 plan types provide average CTV V95% greater than 99.5%, with the non-RO (99.8%) plans slightly higher than the SCT-RO (99.5%) or pMCT-RO (99.6%) plans.

Target and normal tissue D_{max} on the nominal plans and QACTs

In some patients, hot spots were observed on QACT image set. Table 1 lists the pPTV and NT D_{max} of the non-RO, SCT-RO, and pMCT-RO plans on the planning CT, and the highest value of the D_{max} on the 3 to 5 weekly QACTs for each patient. Nominal plans created with all 3 methods had D_{max} no greater than 110.8%, and the volumes receiving 105.0% of the prescription dose were usually confined to small islands. On the nominal plan, D_{max} to pPTV was always greater than D_{max} to the normal tissues.

For doses recalculated on QACTs, the non-RO plans revealed D_{max} up to 144.4% in normal tissue and 130.2% in target. For the SCT-RO plans, D_{max} values on QACTs were greatly reduced from the non-RO plans to 116.9% in normal tissue and 112.4% in pPTV. Nine of the 15 patients had a D_{max} no greater than 110.0%; no patient had D_{max} above 116.9%. For the pMCT-RO plans, on the other hand, all doses calculated on the QACTs were no greater than 110.7% for pPTV and 109.1% for normal tissue.

Figure 2 shows the dose distribution for patient 2 on the planning CT (a-c) and QACT (d-f), and the dose profiles (g-i) for the 3 planning methods. On the QACT, the maximum dose is 131.6% (in normal tissue) for non-RO plan, 115.3% (in normal tissue) for SCT-RO plan, and 109.2% (in pPTV) for the pMCT-RO plan.

Figure 3g-l compares the pPTV and NT D_{max} on all QACTs, and Table 2 indicates both SCT-RO and pMCT-RO methods lowered the pPTV and normal tissue D_{max} compared with the non-RO plans. The pPTV D_{max} averaged over all 67 QACTs was reduced from 110.7% ± 5.8% for the non-RO plans to 108.4% ± 1.4% and 107.8% ± 1.0% for the SCT-RO and pMCT-RO plans, respectively. Furthermore, both SCT-RO and pMCT-RO methods reduced the D_{max} to the NT for the non-RO plans (114.3% ± 9.1%), with the pMCT-RO further decreased it to 107.3% ± 1.0% from 108.9% ± 2.0% for the SCT-RO plans.

The increase of D_{max} to the normal tissue on the QACTs from the nominal plan was also calculated, and Figure 3m-o shows the histogram for each method. The NT D_{max} in increased up to 17.7 Gy for non-RO plans, 5.3 Gy for SCT-RO plans, and 1.7 Gy for the p-4D plans.

Dose to OAR and normal tissues on the nominal plans

As illustrated in Figure E1 (available online at https://doi.org/10.1016/j.adro.2019.12.003), the V90% to the rectum is largely comparable among the 3 plans with the

Table 2 Average (standard deviation) values of non-RO, SCT-RO, and pMCT-RO doses calculated on the 67 QACT images for the 15 patients and the *P* values of paired 2-tail *t* test between the 3 plan types

Parameter	non-RO	SCT-RO	pMCT-RO	*P* value*	*P* value†	*P* value‡
CTV $V_{95\%}$ (%)	99.8 (0.4)	99.5 (0.6)	99.6 (0.5)	.000	.000	.289
CTV $D_{95\%}$ (%)	100.1 (0.5)	100.0 (0.7)	100.0 (0.5)	.317	.631	.279
pPTV D_{max} (%)	110.7 (5.8)	108.4 (1.4)	107.8 (1.0)	.001	.000	.009
Normal tissue D_{max} (%)	114.3 (9.1)	108.9 (2.0)	107.3 (1.0)	.000	.000	.000
Rectum D_{max} (%)	107.5 (5.4)	105.7 (1.5)	105.2 (1.5)	.005	.000	.001
Rectum $V_{90\%}$ (%)	29.6 (13.9)	23.8 (12.9)	24.4 (13.8)	.000	.000	.220
Bladder D_{max} (%)	104.8 (1.5)	106.3 (1.3)	105.5 (1.4)	.000	.001	.000
Bladder $V_{100\%}$ (%)	15.6 (8.5)	12.9 (8.5)	13.4 (8.7)	.001	.008	.001

Abbreviations: CTV = clinical target volumes; D_{max} = maximum point dose; non-RO = without robustness optimization; pMCT-RO = pseudomultiple computed tomography robustness optimization; pPTV = proton planning target volume; QACT = quality assurance computed tomographic scans; SCT-RO = single computed tomography robustness optimization.

* Comparison of SCT-RO plans with non-RO plans.

† Comparison of pMCT-RO plans with non-RO plans.

‡ Comparison of pMCT-RO plans with SCT-RO plans.

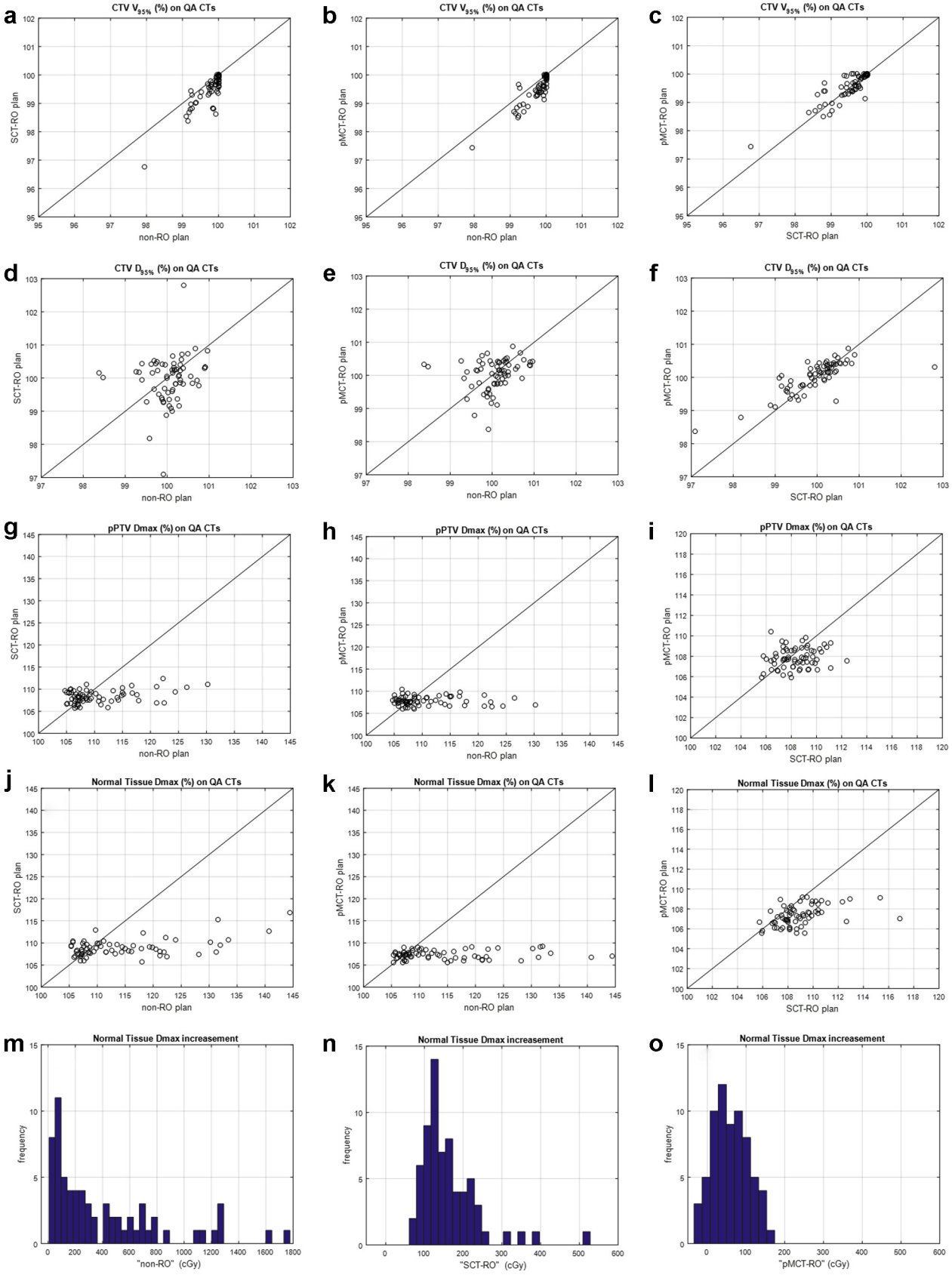

Figure 3 Clinical target volumes (CTV) V95%, CTV D95%, proton planning target volume (pPTV) maximum point dose (D_{max}), and normal tissue D_{max} values on all 67 quality assurance computed tomographic scans plotted with respect to the planning methods (a-l). The solid lines indicate the values are the same for the 2 methods. The histograms of the normal tissue D_{max} increased from the nominal plan to the quality assurance computed tomographic scans are plotted in (m-o) for the 3 planning methods.

non-RO plan D_{max} values slightly lower in selected patients. Similarly, the V100% to the bladder is comparable among the 3 plans, although the non-RO plan bladder D_{max} was slightly lower for some patients. However, the NT_p volume receiving the prescription dose or higher is substantially higher for the non-RO plans (93.2 ± 45.3 mL, mean ± standard deviation), compared with either the SCT-RO plans (19.7 ± 9.7 mL) or the pMCT-RO plans (19.5 ± 6.5 mL); and the NT_c volume receiving prescription dose or higher is also higher for the non-RO plans (502.6 ± 117.6 mL) than the SCT-RO plans (300.3 ± 42.8 mL) and the pMCT-RO plans (287.7 ± 38.5 mL).

Dose to OAR on the QACTs

Table 2 and Fig 4 compare the rectum and bladder dose parameters on the 67 QACTs among different planning methods. The rectum V90%, rectum D_{max}, and bladder V100% were lowered, but the bladder D_{max} was increased when using either RO method. Although there is no statistical difference of the rectum V90% between the 2 RO methods, the bladder V100% was 0.5% higher for the pMCT-RO plans (13.4 ± 8.7%) than the SCT-RO plans (12.9 ± 8.5%), and the bladder D_{max} was 0.8% lower for the pMCT-RO plans (105.5 ± 1.4%) than the SCT-RO plans (103.3 ± 1.3%). The average D_{max} for all 3 planning methods are less than 107.5% for rectum and 105.5% for bladder.

Discussion

The observation of concerning hotspots that developed in normal tissues as a consequence of random anatomic changes are detailed in Table 1. Figure 2 is an example (patient 2) of bowel filling change as seen on the first weekly QACT image. As a result, the 2 lateral beams overrange into each other and created a hot spot (131.6% of the prescription dose) in the bowel area. These hot spots were usually confined in very small volumes and changed locations from week to week owing to the randomness in anatomic changes. No patients were replanned because this variance could occur just as likely with a new plan using the same methodology. These concerns prompted the present study of a novel technique that could account for random tissue density changes unaccounted for by standard planning approaches.

Robustness optimization has been proven to be beneficial for intensity modulated proton therapy robustness by reducing high dose gradient in individual fields in the target[19] and by finding a fluence map solution to make the dose cloud to move with the anatomic geometry.[20] By including a setup up error of 5 mm and range uncertainty of ±3.5% (the SCT-RO method), the hot spots on the QACTs were greatly decreased, all below 117.0% as seen in Table 1. Although SCT-RO only includes the patient setup and proton range uncertainties, its capability of decreasing the individual beam's dose gradient indirectly reduced the uncertainty caused by patient anatomy variation to a partial degree. As shown in Figure 2, that SCT-RO methodology decreased hot spots from as much as 131.6% to 115.3% in comparison to non-RO planning.

To further improve the plan robustness against anatomic density changes, it is beneficial to include this uncertainty directly in the robustness optimization process. Taking the synthetic images into consideration during RO further decreased the degradation of delivered dose to the patient due to anatomic change. In Figure 3, hot spots observed with non-RO or SCT-RO methods disappeared when pMCT-RO techniques were used. In fact, the doses recalculated on all 67 QACTs for all 15 patients showed maximum dose no greater than 110.7%.

On the nominal plans, the pPTV D_{max} was higher than NT D_{max} for all 3 methods, as seen in Table 1. On the other hand, the NT D_{max} on the QACTs was higher than pPTV D_{max} for 13 patients with the non-RO method, for 10 patients with SCT-RO method, and only for 2 patients with the pMCT-RO method. Despite the same optimization objectives been used, the pPTV D_{max} was 0.9% higher for the SCT-RO method than the pMCT-RO method. This may have contributed to the slightly higher pPTV D_{max} observed on the QACTs. On the nominal plans, the NT D_{max} for SCT-RO plans was 0.8% lower than for the pMCT-RO plans; however, on the QACTs, the NT D_{max} was 1.5% higher for the SCT-RO plans than the pMCT-RO plans. It is worth pointing out that the SCT-RO method already significantly reduced the NT D_{max} on the QACTs, using additional CTs to simulate bowel density variation further reduced the hot spot to the normal tissue.

Our pMCT-RO method does not require additional patient CT scans. Instead, we simulate the potential bowel filling with 2 extreme scenarios: all air (CT_air) and all tissue (CT_tissue). Its implementation is relatively straightforward but does require the ability to take multiple CT data sets into account during RO. A commercial 4D RO optimizer was used in this work.

In non-RO plans, an increase in robustness can be achieved with increased dosimetric margins that inherently increase the dose to abutting structures. To test whether the increased robustness in the RO plans comes with a dosimetric cost, we compared the dosimetry of the nominal plans. As illustrated in Fig E1, the RO plans resulted in similar or even less dose to abutting structures. One explanation is that, without RO, a uniform geometric expansion of the CTV is required to ensure CTV coverage from uncertainties. This consequently increases the dose to the normal tissue. Robust optimization, on the other hand, only covers CTV with sufficient margin for each beam and therefore minimizes irradiation of nontarget tissue. Similarly, Liu et al, reported robust optimization provides robust target coverage without sacrificing normal tissue sparing.[21]

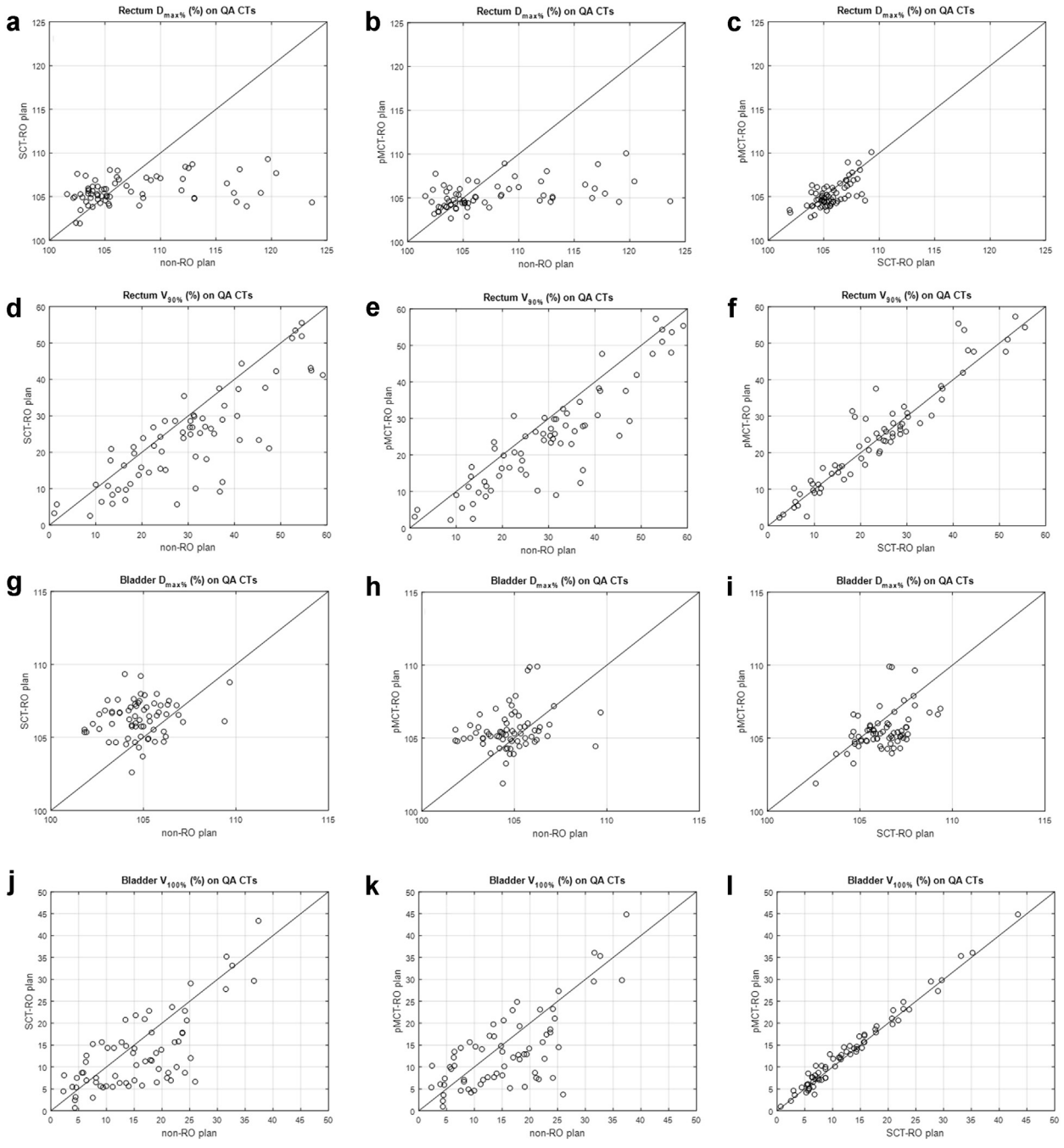

Figure 4 Rectum maximum point dose (D_{max}), rectum V90%, bladder D_{max}, and bladder D100% dose values on all 67 quality assurance computed tomographic scans plotted with respect to the planning methods. The solid lines indicate the values are the same for the 2 methods.

Doses calculated on the QACTs indicates all 3 methods provided sufficient dose coverage to the CTV. The non-RO plans designed to cover a pPTV resulted in a statistically significant, but clinically insignificant, improvement of the CTV V95% than the SCT-RO and pMCT-RO plans. However, the dosimetric cost of covering a pPTV is the substantially larger amount of normal tissue receiving high doses. Both SCT-RO and pMCT-RO plans had lower rectum D_{max}, rectum D90%, and bladder V100% on the QACTs than the non-RO plans, further demonstrating the effectiveness of robust optimization.

One limitation of our pMCT-RO method is that applying density variations of the bowel structures does not directly account for potential interfractional motion of such structures. The combination of the setup error with the additional images does include a shift of the bowel structures with assigned density by 5 mm in all directions; this may have helped the pMCT-RO method further reduced the hot spots in QACTs; however, more rigorous

analysis or experiment is required to establish the correlation.

Including 3 CT images also increased the plan optimization time by a factor of 3. For the plans created in this study, the average plan optimization time was around 30 minutes for SCT-RO plans and 90 minutes for the pMCT-RO plans in a clinical treatment planning system.

We have implemented the pMCT-RO planning technique for all prostate pelvic node pencil beam scanning treatments since July of 2017. Based on the consistently improved plan robustness on QACTs through the pMCT-RO method, we have decreased QACT frequency from weekly scans to 2 total scans during the course of treatment for this patient population.

Conclusions

Undesired dose heterogeneity owing to random anatomic changes during pelvic proton radiation therapy can be substantially mitigated by using the traditional (setup and range uncertainties) robust optimization. The use of multiple CT scans to mimic anticipated anatomic variations may further reduce the maximum dose to normal tissues as evaluated on the QACTs. The pMCT-RO method outlined in this article comes at no extra cost in terms of additional patient CT scans. The method has been implemented clinically since 2017 in our center.

Supplementary data

Supplementary material for this article can be found at https://doi.org/10.1016/j.adro.2019.12.003.

References

1. Pan HY, Jiang J, Shih YT, et al. Adoption of radiation technology among privately insured nonelderly patients with cancer in the United States, 2008 to 2014: A claims-based analysis. *J Am Coll Radiol*. 2017;14:1027-1033.
2. Aizer AA, Yu JB, McKeon AM, et al. Whole pelvic radiotherapy versus prostate only radiotherapy in the management of locally advanced or aggressive prostate adenocarcinoma. *Int J Radiat Oncol Biol Phys*. 2009;75:1344-1349.
3. Schardt D, Elsässer T, Schulz-Ertner D. Heavy-ion tumor therapy: Physical and radiobiological benefits. *Rev Mod Phys*. 2010;82:383-425.
4. Dowdell SJ, Metcalfe PE, Morales JE, et al. A comparison of proton therapy and IMRT treatment plans for prostate radiotherapy. *Australas Phys Eng Sci Med*. 2008;31:325-331.
5. Widesott L, Pierelli A, Fiorino C, et al. Helical tomotherapy vs intensity-modulated proton therapy for whole pelvis irradiation in high-risk prostate cancer patients: Dosimetric, normal tissue complication probability, and generalized equivalent uniform dose analysis. *Int J Radiat Oncol Biol Phys*. 2011;80:1589-1600.
6. Allen AM, Pawlicki T, Dong L, et al. An evidence based review of proton beam therapy: The report of ASTRO's emerging technology committee. *Radiother Oncol*. 2012;103:8-11.
7. Chera BS, Vargas C, Morris CG, et al. Dosimetric study of pelvic proton radiotherapy for high-risk prostate cancer. *Int J Radiat Oncol Biol Phys*. 2009;75:994-1002.
8. Vees H, Dipasquale G, Nouet P, et al. Pelvic lymph node irradiation including pararectal sentinel nodes for prostate cancer patients: Treatment optimization comparing intensity modulated x-rays, volumetric modulated arc therapy, and intensity modulated proton therapy. *Technol Cancer Res Treat*. 2015;14:181-189.
9. Busch K, G Andersen A, Casares-Magaz O, et al. Evaluating the influence of organ motion during photon vs proton therapy for locally advanced prostate cancer using biological models. *Acta Oncol*. 2017;56:839-845.
10. Lomax AJ. Intensity modulated proton therapy and its sensitivity to treatment uncertainties 1: The potential effects of calculational uncertainties. *Phys Med Biol*. 2008;53:1027-1042.
11. Haganetti H. Range uncertainties in proton therapy and the role of Monte Carlo simulations. *Phys Med Biol*. 2012;57:R99.
12. Langen K, Zhu M. Concepts of PTV and robustness in passively scattered and pencil beam scanning proton therapy. *Semin Radiat Oncol*. 2018;28:248-255.
13. Tang S, Deville C, Tochner Z, et al. Impact of intrafraction and residual interfraction effect on prostate proton pencil beam scanning. *Int J Radiat Oncol Biol Phys*. 2014;90:1186-1194.
14. Thornqvist S, Muren LP, Bentzen L, et al. Degradation of target coverage due to interfraction motion during intensity modulated proton therapy of prostate and elective targets. *Acta Oncol*. 2013;52:521-527.
15. Wang X, Li H, Zhu XR, et al. Multiple-CT optimization of intensity modulated proton therapy: Is it possible to eliminate adaptive planning? *Radiother Oncol*. 2018;128:167-173.
16. van de Water S, Albertini F, Weber DC, et al. Anatomical robust optimization to account for nasal cavity filling variation during intensity-modulated proton therapy: A comparison with conventional and adaptive planning strategies. *Phys Med Biol*. 2018;63:025020.
17. Fredriksson A, Forsgren A, Hardemark B. Minimax optimization for handling range and setup uncertainties in proton therapy. *Med Phys*. 2011;38:1672-1684.
18. Liu W, Schild SE, Chang JY, et al. Exploratory study of 4D versus 3D robust optimization in intensity modulated proton therapy for lung cancer. *Int J Radiat Oncol Biol Phys*. 2016;95:523-533.
19. Albertini F, Hug EB, Lomax AJ. Is it necessary to plan with safety margins for actively scanned proton therapy? *Phys Med Biol*. 2011;56:4399-4413.
20. Liu W, Li Y, Li X, et al. Influence of robust optimization in intensity modulated proton therapy with different dose delivery techniques. *Med Phys*. 2012;39:3089-3101.
21. Liu W, Zhang X, Li Y, et al. Robust optimization of intensity modulated proton therapy. *Med Phys*. 2012;39:1079-1091.